

# Machine Learning Analysis Reveals Abnormal Static and Dynamic Low-Frequency Oscillations Indicative of Long-Term Menstrual Pain in Primary Dysmenorrhea Patients

Shao-Gao Gui<sup>1,2,\*</sup>  
Ri-Bo Chen<sup>2,\*</sup>  
Yu-Lin Zhong<sup>1</sup>  
Xin Huang<sup>1</sup>

<sup>1</sup>Department of Ophthalmology, Jiangxi Provincial People's Hospital Affiliated to Nanchang University, Nanchang, 330006, Jiangxi, People's Republic of China;

<sup>2</sup>Department of Radiology, Jiangxi Provincial People's Hospital Affiliated to Nanchang University, Nanchang, 330006, Jiangxi, People's Republic of China

\*These authors contributed equally to this work

**Background:** Previous neuroimaging studies demonstrated that patients with primary dysmenorrhea (PD) exhibited dysfunctional resting-state brain activity. However, alterations of dynamic brain activity in PD patients have not been fully characterized.

**Purpose:** Our study aimed to assess the effect of long-term menstrual pain on changes in static and dynamic neural activity in PD patients.

**Material and Methods:** Twenty-eight PD patients and 28 healthy controls (HCs) underwent resting-state magnetic resonance imaging scans. The amplitude of low-frequency fluctuations (ALFF) and dynamic ALFF was used as classification features in a machine learning approach involving a support vector machine (SVM) classifier.

**Results:** Compared with the HC group, PD patients showed significantly increased ALFF values in the right cerebellum\_crus2, right rectus, left supplementary motor area, right superior frontal gyrus, right supplementary motor area, and left superior frontal medial gyrus. Additionally, PD patients showed significantly decreased ALFF values in the right middle temporal gyrus and left thalamus. PD patients also showed significantly increased dALFF values in the right fusiform, Vermis\_10, right middle temporal gyrus, right putamen, right insula, left thalamus, right precentral gyrus, and right postcentral gyrus. Based on ALFF and dALFF values, the SVM classifier achieved respective overall accuracies of 96.36% and 85.45% and respective areas under the curve of 1.0 and 0.95.

**Conclusion:** PD patients demonstrated abnormal static and dynamic brain activities that involved the default mode network, sensorimotor network, and pain-related subcortical nuclei. Moreover, ALFF and dALFF may offer sensitive biomarkers for distinguishing patients with PD from HCs.

**Keywords:** primary dysmenorrhea, amplitude of low-frequency fluctuations, support vector machine

Correspondence: Xin Huang  
Department of Ophthalmology, Jiangxi Provincial People's Hospital Affiliated to Nanchang University, No. 152, Ai Guo Road, Dong Hu District, Nanchang, 330006, Jiangxi, People's Republic of China  
Tel +86 15879215294  
Email 334966891@qq.com

## Introduction

Primary dysmenorrhea (PD) is one of the most frequent gynecological diseases, characterized by persistent abdominal pain during the menstrual period. The incidence of PD in university students is 41.7% in China.<sup>1</sup> There is increasing evidence that PD patients have both abdominal pain and psychological problems and a nutraceutical approach to female complaints has increased during the last years.<sup>2,3</sup> Kabukcu et al reported that PD may be associated with psychiatric

distress.<sup>4</sup> However, the effects of long-term menstrual pain on psychological disorder-related neural activity in PD patients remain unclear.

The resting-state fMRI technique has provided a robust understanding of neurophysiological mechanisms in PD patients. Zhang et al demonstrated that PD patients showed decreased ALFF in the posterior lobe of the right cerebellum and right middle temporal gyrus, compared with HCs.<sup>5</sup> Zhang et al demonstrated that PD patients exhibited abnormal cerebral blood flow in the default mode network, compared with HCs.<sup>6</sup> Furthermore, Liu found that PD patients showed abnormal connectivity between the caudal anterior cingulate cortex (ACC) and both the primary somatosensory cortex and the medial prefrontal cortex.<sup>7</sup> Lee et al demonstrated that PD patients showed increased theta activity in the parahippocampal gyrus, insula, and cingulate gyrus during the menstrual period.<sup>8</sup> Although these findings have revealed changes in brain activity specific to pain and related brain regions in PD patients, they focused on the resting-state features of blood-oxygenation-level dependent (BOLD) signaling, with the assumption that BOLD signaling is stationary during the acquisition period. However, the effects of long-term menstrual pain on dynamic intrinsic brain activity remain unknown.

Increasing numbers of neuroimaging studies have been performed with the assumption of temporal variability in BOLD signal correlations during the typical duration (a few minutes) of a resting-state scan.<sup>9,10</sup> Recently, dynamic ALFF was successfully used to investigate the temporal variability of brain activity in patients who were smokers,<sup>11</sup> patients with primary insomnia,<sup>12</sup> and patients with Parkinson's disease.<sup>13</sup> In contrast to task MRI method, this technique does not require the participants to perform any task during scanning and the ALFF method had high spatial resolution. However, it remains poorly understood whether changes in dynamic spontaneous brain activity occur in PD patients. Additionally, the support vector machine (SVM) method has been used in MRI classification to detect biomarkers on the basis of neuroimaging data.

This study aimed to determine whether PD patients exhibited dysfunctional dynamic intrinsic brain activity. Additionally, machine learning techniques were applied to investigate whether ALFF and dALFF values could serve as sensitive biomarkers to distinguish patients with PD from HCs. Our findings might offer insights into the

neural mechanisms of long-term menstrual pain in PD patients.

## Materials and Methods

### Participants

A case-control study, 28 PD patients (28 women; mean age, 24.25±1.00 years) and 28 HCs (28 women; mean age, 24.46±1.31 years) were enrolled in Jiangxi Provincial People's Hospital Affiliated to Nanchang University China during 1 September 2020 to 1 January 2021, matched for age, sex, and education, participated in this study.

The diagnostic criteria of PD patients were as follows: 1) childless, right-handed women; 2) with menstrual cycle of 21–35 days; a3) course of menstrual pain lasting longer than 6 months; 4) an average visual analogue score (VAS) of menstrual pain of greater than or equal to 40 (0=no pain sensation, 100=the worst pain sensation) in this study.

All HCs met the following criteria: 1) no history of abdominal pain; 2) presence of pelvic organic diseases.

### Ethical Statement

The studies involving human participants were reviewed and approved by Declaration of Helsinki and was approved by the medical ethics committee of the Jiangxi Provincial People's Hospital Affiliated to Nanchang University. The research program was approved by the institutional review board of Jiangxi Provincial People's Hospital Affiliated to Nanchang University. All subjects signed an informed consent form.

### MRI Acquisition

MRI scanning was performed on a 3-tesla magnetic resonance scanner (Discovery MR 750W system; GE Healthcare, Milwaukee, WI, USA) with eight-channel head coil.

### fMRI Data Processing

All preprocessing was performed using the toolbox for Data Processing & Analysis of Brain Imaging (DPABI, <http://www.rfmri.org/dpabi>),<sup>14</sup> briefly the following steps:<sup>15</sup> 1) discard first 10 volumes, 2) slice timing effects and motion corrected. 3) Individual 3D-BRAVO images were registered to the mean fMRI data.<sup>16</sup> 4) regress out several covariate (six head motion parameters, mean framewise displacement (FD), global

**Table 1** Demographics and Visual Measurements Between Two Groups

	PD Group	HC Group	T-values	P-values
Gender (female)	28	28	N/A	N/A
Age (years)	24.25±1.00	24.46±1.31	-0.684	0.497
Handedness	28 R	28 R	N/A	N/A
Education (years)	15.00±0.72	14.67±0.98	1.396	0.169
Visual analog scores	54.2±37.4	N/A	N/A	N/A

**Note:** Independent t-test was applied to assess the clinical features (means ± SD).

**Abbreviations:** PD, primary dysmenorrhea; HC, health control.

brain signal, and averaged signal from white matter signal and cerebrospinal fluid). 5) Data with linear trend were removed, and temporal band-pass was filtered (0.01–0.08 Hz).<sup>17</sup>

## ALFF Computing

To calculate ALFF, we calculate the smoothed signal of each voxel from time domain to frequency domain via Fast Fourier Transform (FFT) to obtain the power spectrum.

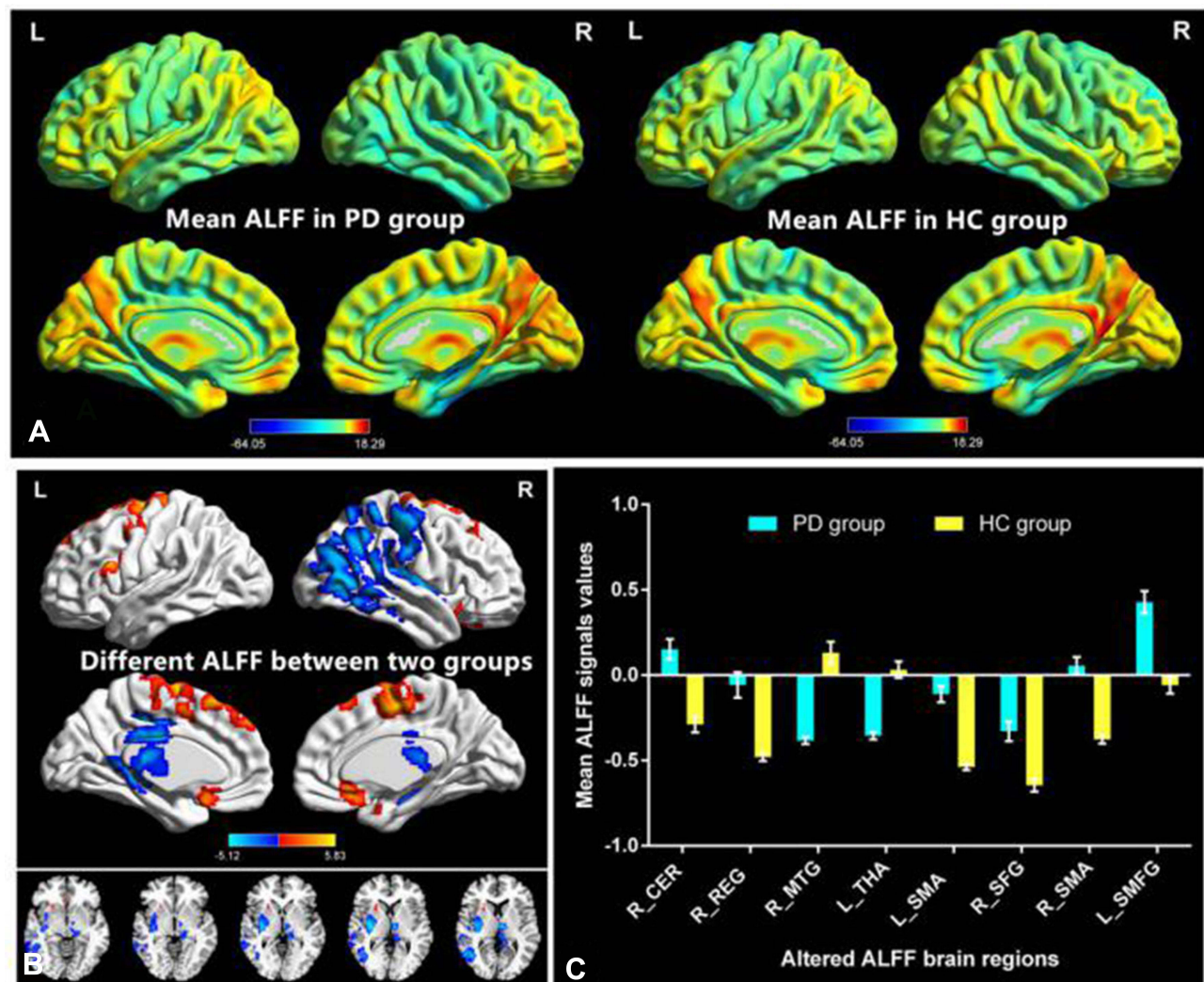


**Figure 1** Distribution patterns of ALFF variance (window lengths (30 TRs [60s]) were observed at the group level in PD and HC groups in the typical frequency band (0.01–0.08 Hz). (A) Different ALFF values between two groups. (B) The mean values of altered ALFF were shown with a histogram. (C).

**Abbreviations:** ALFF, amplitude of low-frequency fluctuation; PD, primary dysmenorrhea; HC, health controls; L, left; R, right; CER, cerebellum\_crus2; REG, rectus; SMA, supplementary motor area, right SFG, superior frontal gyrus, right supplementary motor area, left SMFG, superior frontal medial gyrus; right MTG, middle temporal gyrus; THA, thalamus.

**Table 2** Different ALFF Values Between Two Groups

Condition	Brain Regions	BA	Peak T-Scores	MNI Coordinates (x, y, z)	Cluster Size (Voxels)
PD>HC	Cerebellum_Crus2_R	–	4.3423	27 –84 –24	189
PD>HC	Rectus_R	–	4.1772	24 18 –9	183
PD<HC	Temporal_Mid_R	–	–5.1151	54 –63 9	2038
PD<HC	Thalamus_L	–	–4.835	–6 –15 27	400
PD>HC	Supp_Motor_Area_L	–	5.8345	–12 –3 63	515
PD>HC	Frontal_Sup_R	8	3.4208	18 30 39	45
PD>HC	Supp_Motor_Area_R	6	5.0168	15 –15 66	333
PD>HC	Frontal_Sup_Medial_L	8	4.2658	–3 30 57	109

**Note:** The statistical threshold was set at the voxel level with  $p < 0.01$  for multiple comparisons using Gaussian random-field theory.

**Abbreviations:** ALFF, amplitude of low-frequency fluctuation; PD, primary dysmenorrhea; HC, health control; R, right; L, left; GRF, Gaussian random field.

## dALFF Computing

A sliding window approach was used to compute the dALFF.<sup>18</sup>

For sliding-window approach, a window size of 50 TRs (100 s) and a window shifted by 10 TRs were selected.<sup>19</sup>

## Clinical Evaluation

Clinical data were recorded, including age, sex, education levels.

## Statistical Analysis

Independent-sample *t*-test was used to investigate the clinical features between two groups.

One-sample *t*-test was used to group patterns of zALFF and zdALFF maps. Two-sample *t*-test was used to assess two group differences in the zALFF and zdALFF maps. Gaussian random field (GRF) method was used to correct for multiple comparisons and regressed covariates of age and sex and FD (two-tailed, voxel-level  $P < 0.01$ , GRF correction, cluster-level  $P < 0.05$ ).

## Support Vector Machine Analysis

The SVM algorithm was performed based on the Pattern Recognition for Neuroimaging Toolbox (PRoNTo) software<sup>20</sup> with the following steps: 1) the ALFF and dALFF maps served as classification feature. 2) The leave-one-out cross-validation (LOOCV) technique was used for SVM method. 3) For classification, the permutation test was used to investigate assess the total accuracy of this classification.<sup>21</sup> The total accuracy, specificity, sensitivity, and area under the receiver operating characteristic curve (ROC) were determined to assess the classification performance of the machine learning model.

## Verification Analyses

Two different window lengths (30 TRs [60 s] and 100 TRs [200 s]) were calculated in the validation analysis.

## Results

### Clinical Features

There were no any differences in age and gender between the two groups. ( $p > 0.05$ ) (Table 1).

### ALFF Differences

The group mean of ALFF maps of the PD and HC (Figure 1A). Compared to the HC group, PD patients showed significant increased ALFF values in the right cerebellum\_crus2, right rectus, left supplementary motor area, right superior frontal gyrus, right supplementary motor area, left superior frontal medial gyrus. Meanwhile, PD patients showed significant decreased ALFF values in the right middle temporal gyrus and left thalamus (Figure 1B and Table 2). The mean values of altered ALFF maps are shown with a histogram (Figure 1C).

### Dynamic ALFF Differences

The group mean of dALFF maps of the PD and HCs (Figure 2A). PD patients showed significant increased dALFF values in the right fusiform, Vermis\_10, right middle temporal gyrus, right putamen, right insula, left thalamus, right precentral gyrus and right postcentral gyrus and left precuneus (Figure 2B and Table 3). The mean values of altered dALFF maps are shown with a histogram (Figure 2C).

### SVM Classification Results

The SVM classification reached a total accuracy of 96.36% based on ALFF. The AUC of the classification model was 1.0 based on ALFF. SVM analysis based on ALFF function values of two groups (class 1: patient group; class 2: HC group) (Figure 3A); three-dimensional confusion matrices (Figure 3B); the AUC was 1.0 (Figure 3C); weight maps for SVM models (Figure 3D).



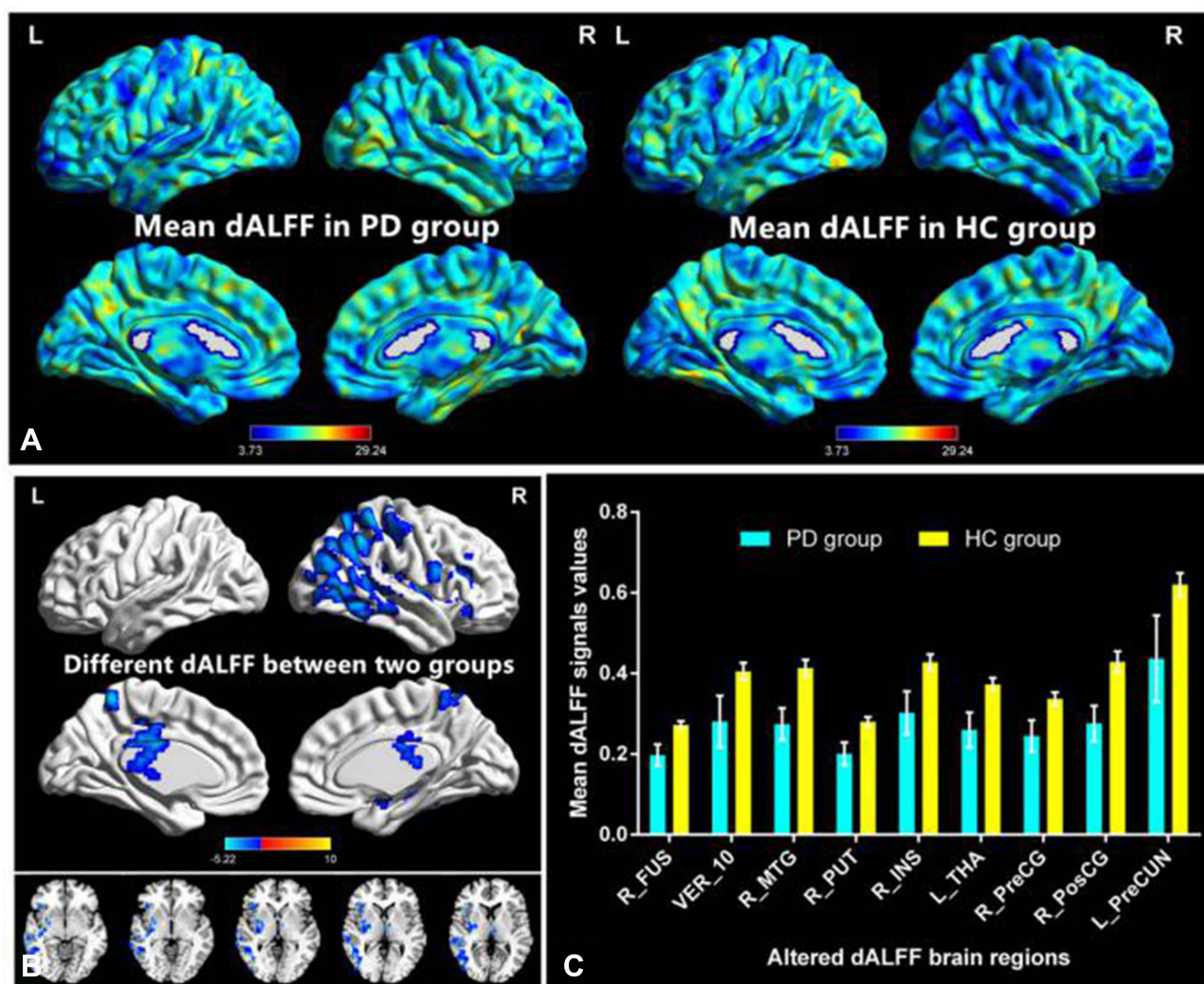


**Figure 2** Distribution patterns of dALFF variance (window lengths (30 TRs [60s]) were observed at the group level in PD and HC groups in the typical frequency band (0.01–0.08 Hz). (A) Different dALFF values between two groups. (B) The mean values of altered dALFF was shown with a histogram. (C). **Abbreviations:** dALFF, dynamic amplitude of low-frequency fluctuation; PD, primary dysmenorrhea; HC, health controls; L, left; R, right; FUS, fusiform; VER, Vermis\_10; MTG, middle temporal gyrus; PUT, putamen; INS, insula; THA, thalamus; PreCG, precentral gyrus; PosCG, postcentral gyrus; PreCUN, precuneus.

The SVM classification reached a total accuracy of 85.45% based on dALFF. The AUC of the classification model was 0.95 based on dALFF. SVM analysis based on dALFF function values of two groups (class 1: patient

**Table 3** Different dALFF Values Between Two Groups

Condition	Brain Regions	BA	Peak TScores	MNI Coordinates (x, y, z)	Cluster Size (Voxels)
PD<HC	Fusiform_R	–	–4.4563	36 –39 –21	99
PD<HC	Vermis_10	–	–4.6151	–12 –42 –27	87
PD<HC	Temporal_Mid_R	–	–4.834	48 –51 0	975
PD<HC	Putamen_R	–	–4.3334	33 –18 0	260
PD<HC	Insula_R	–	–4.089	36 24 3	100
PD<HC	Thalamus_L	–	–4.6586	–3 –15 27	179
PD<HC	Precentral_R	–	–3.8885	60 6 21	40
PD<HC	Postcentral_R	8	–5.2217	33 –60 60	417
PD<HC	Precuneus_L	–	–4.6802	–3 –48 60	65

**Note:** The statistical threshold was set at the voxel level with  $p < 0.01$  for multiple comparisons using Gaussian random-field theory.

**Abbreviations:** dALFF, dynamic amplitude of low-frequency fluctuation; PD, primary dysmenorrhea; HC, health control; R, right; L, left; GRF, Gaussian random field.

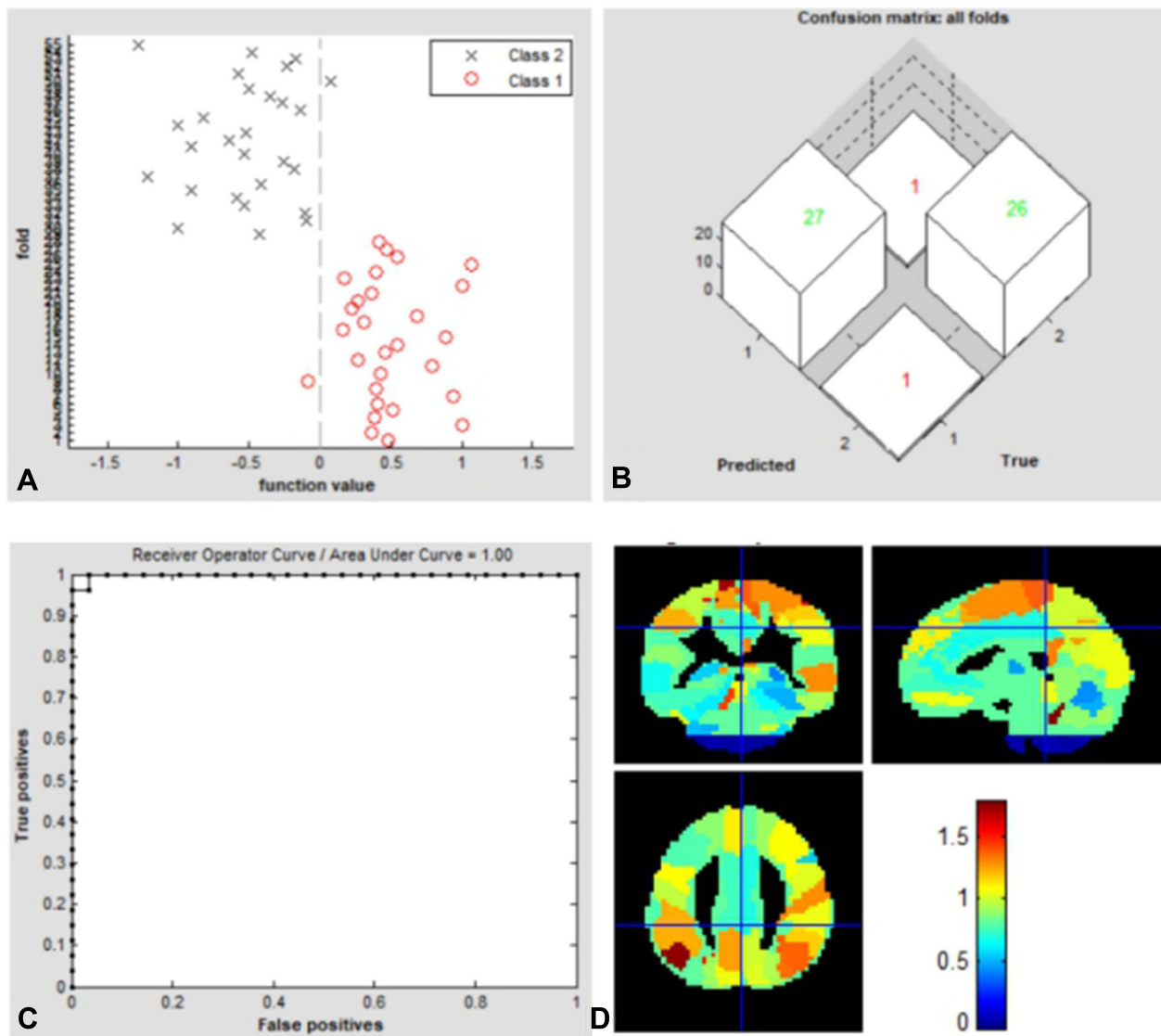


**Figure 3** SVM analysis based on ALFF function values of two groups (class 1: patient group; class 2: HC group) (A); three-dimensional confusion matrices (B); the AUC was 1.0 (C); weight maps for SVM models (D).

**Abbreviations:** SVM, support vector machine; ALFF, amplitude of low-frequency fluctuations; AUC, area under the curve.

group; class 2: HC group) (Figure 4A); three-dimensional confusion matrices (Figure 4B); the AUC was 0.95 (Figure 4C); weight maps for SVM models (Figure 4D).

## Verification Analyses

Distribution patterns of dALFF variance (window lengths (30 TRs [60s]) were observed at the group level in PD and HC groups (Figure S1A). Compared with HC group, the PD group showed significant decreased dALFF values in the right fusiform, right middle temporal gyrus, right superior temporal gyrus, left thalamus, right precentral

gyrus and right postcentral gyrus (Figure S1B and Table S1). The mean values of altered dALFF between were shown with a histogram (Figure S1C).

Distribution patterns of dALFF variance (window lengths (100 TRs [200s]) were observed at the group level in PD and HC groups (Figure S2A). Compared with HC group, the PD group showed significant decreased dALFF values in the right middle temporal gyrus, right inferior parietal lobe and right postcentral gyrus (Figure S2B and Table S2). The mean values of altered dALFF between the two groups were shown with a histogram (Figure S2C).

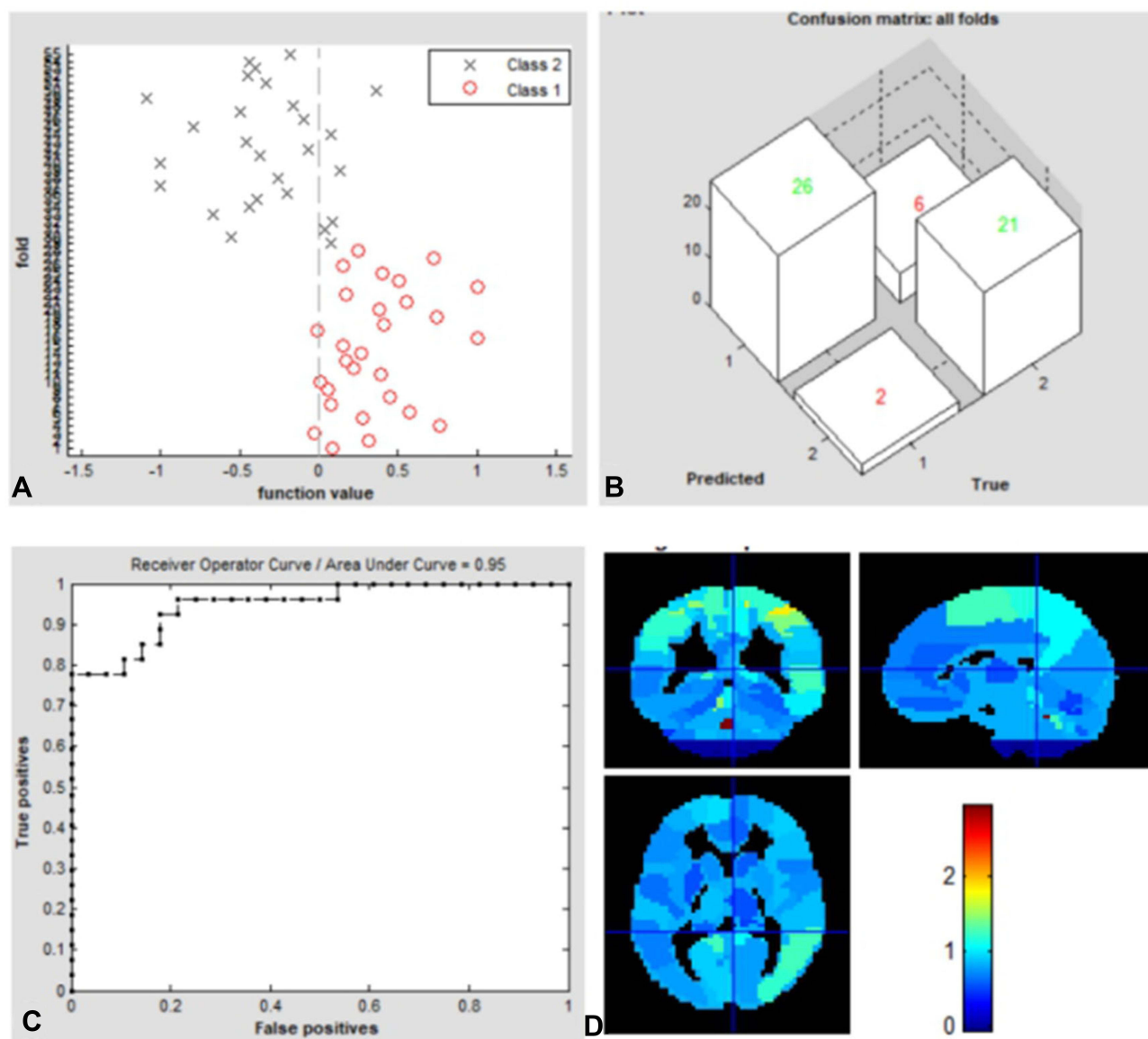


**Figure 4** SVM analysis based on dALFF/function values of two groups (class 1: patient group; class 2: HC group) (A); three-dimensional confusion matrices (B); the AUC was 0.95 (C); weight maps for SVM models (D).

**Abbreviations:** SVM, support vector machine; dALFF, dynamic amplitude of low-frequency fluctuations; AUC, area under the curve.

## Discussion

Our study aimed to investigate the effects of long-term menstrual pain on changes in static and dynamic ALFF in PD patients. Compared with the HC group, PD patients showed significant increased ALFF values in the right cerebellum\_crus2, right rectus, left supplementary motor area, right superior frontal gyrus, right supplementary motor area, and left superior frontal medial gyrus. Additionally, PD patients showed significantly decreased ALFF values in the right middle temporal gyrus and left thalamus. PD patients also showed significantly increased

dALFF values in the right fusiform, Vermis\_10, right middle temporal gyrus, right putamen, right insula, left thalamus, right precentral gyrus, and right postcentral gyrus. Based on ALFF and dALFF values, the SVM classifier achieved respective overall accuracies of 96.36% and 85.45% and respective AUCs of 1.0 and 0.95.

Our study demonstrated that PD patients had significant changes in ALFF and dALFF values in the right middle temporal gyrus and the left superior frontal medial gyrus; these are core brain regions within the default mode network (DMN). Previous studies indicated that chronic

pain appears to reorganize the dynamics of the DMN.<sup>22–24</sup> Liu et al reported DMN-related abnormalities in PD patients, which might reflect the neurophysiological mechanism of this disease.<sup>25</sup> Consistent with these previous findings, we observed that PD patients had significant changes in ALFF and dALFF values in the DMN-related brain regions, which might reflect attention and mental flexibility deficits in PD patients.

The cerebellum has an important role in motor processing. Previous neuroimaging studies demonstrated that the cerebellum is involved in pain or pain modulation.<sup>26,27</sup> Zhang et al demonstrated that PD patients had decreased ALFF in the posterior lobe of the right cerebellum.<sup>5</sup> In accordance with the previous findings, the present study showed that PD patients had increased ALFF values in the right cerebellum\_crus2 and decreased dALFF values in the Vermis\_10. We speculate that higher brain activities in the cerebellum might contribute to long-term menstrual pain in PD patients.

Another important finding was that PD patients showed dysfunction in several subcortical nuclei (eg, right rectus, right putamen, right insula, and left thalamus). Previous neuroimaging studies demonstrated that these subcortical nuclei (ie, putamen, insula, and thalamus) have important roles in pain and pain-related emotional processing.<sup>28–31</sup> Lee et al found that PD patients showed increased theta activity in the right posterior insula during pain processing.<sup>8</sup> Furthermore, Dun et al observed lower gray matter density in the left anterior insula in PD patients, which might reflect the disconnection of pain attention and pain perception networks in these patients.<sup>32</sup> The thalamus is a key region for the transmission of nociceptive information in the central modulation of pain. He et al demonstrated that changes in the white matter of thalamus-SI pathways were present in PD patients; changes in these pathways were closely associated with the degree of menstrual pain experienced by in PD patients.<sup>33</sup> Shilan Quan found that treatment options of PD patients may be expanded from only being able to manage pain in the uterus focusing on the functional/structural modifications of the pain processing system.<sup>34</sup> Thus, we speculate that changes in static and dynamic brain activities in subcortical nuclei might contribute to long-term menstrual pain in PD patients.

In addition, we found that PD patients demonstrated significantly increased ALFF values in the supplementary motor area, whereas they showed significantly decreased dALFF values in the right precentral gyrus and right postcentral gyrus. The sensorimotor network has a critical role

in sensory function and is involved in pain coding.<sup>35,36</sup> Importantly, Wei et al demonstrated that PD patients had adaptive/reactive hyperconnectivity with the sensorimotor cortex during painful menstruation.<sup>37</sup> On the basis of these findings, we presume that long-term pain might contribute to sensorimotor network dysfunction in PD patients.

In our study, the SVM classifier achieved respective overall accuracies of 96.36% and 85.45% and respective AUCs of 1.0 and 0.95. Thus, ALFF and dALFF may offer sensitive biomarkers for distinguishing patients with PD from HCs.

This study had several limitations. First, its small sample size might have reduced its ability to detect more alterations in neuronal activity. Second, the impacts of physiological noise were not completely eliminated, which may have confounded blood oxygen level-dependent signals.

In conclusion, our study showed that PD patients had abnormal static and dynamic brain activities that involved the DMN, sensorimotor network, and pain-related subcortical nuclei. Moreover, ALFF and dALFF could serve as sensitive biomarkers for distinguishing patients with PD from HCs.

## Abbreviation

PD, primary dysmenorrhea; HCs, healthy controls; ALFF, amplitude of low-frequency fluctuations; SVM, support vector machine; dALFF, dynamic amplitude of low-frequency fluctuations; ACC, anterior cingulate cortex; BOLD, blood-oxygenation-level dependent; FD, mean framewise displacement; FFT, Fast Fourier Transform; GRF, Gaussian random field; PRoNT, Pattern Recognition for Neuroimaging Toolbox; LOOCV, leave-one-out cross-validation; ROC, receiver operating characteristic curve; DMN, default mode network.

## Acknowledgments

We acknowledge the assistance provided by the Natural Science Foundation of Jiangxi Province (20192BAB205048) National Nature Science Foundation of China (grant no. 81060080).

## Disclosure

The authors report no conflicts of interest in this work.

## References

1. Hu Z, Tang L, Chen L, et al. Prevalence and risk factors associated with primary dysmenorrhea among Chinese Female University Students: a cross-sectional study. *J Pediatr Adolesc Gynecol.* 2020;33:15–22.



2. Gagua T, Tkeshelashvili B, Gagua D, et al. Assessment of anxiety and depression in adolescents with primary dysmenorrhea: a case-control study. *J Pediatr Adolesc Gynecol.* 2013;26:350–354.
3. De Francis P, Colacurci N, Riemma G, Conte A, Pittana E, Guida MA. Nutraceutical approach to menopausal complaints. Schiattarella A. *Medicina (Kaunas).* 2019;55(9):544.
4. Kabukcu C, Kabukcu Basay B, Basay O. Primary dysmenorrhea in adolescents: association with attention deficit hyperactivity disorder and psychological symptoms. *Taiwan J Obstet Gynecol.* 2021;60:311–317.
5. Zhang YN, Huo JW, Huang YR, et al. Altered amplitude of low-frequency fluctuation and regional cerebral blood flow in females with primary dysmenorrhea: a resting-state fMRI and arterial spin labeling study. *J Pain Res.* 2019;12:1243–1250.
6. Zhang YN, Huang YR, Liu JL, et al. Aberrant resting-state cerebral blood flow and its connectivity in primary dysmenorrhea on arterial spin labeling MRI. *Magn Reson Imaging.* 2020;73:84–90.
7. Liu P, Liu Y, Wang G, et al. Changes of functional connectivity of the anterior cingulate cortex in women with primary dysmenorrhea. *Brain Imaging Behav.* 2018;12:710–717.
8. Lee PS, Low I, Chen YS, et al. Encoding of menstrual pain experience with theta oscillations in women with primary dysmenorrhea. *Sci Rep.* 2017;7:15977.
9. Chang C, Glover GH. Time-frequency dynamics of resting-state brain connectivity measured with fMRI. *Neuroimage.* 2010;50:81–98.
10. Ma Z, Zhang N. Temporal transitions of spontaneous brain activity. *Elife.* 2018;7:e33562.
11. Xue T, Dong F, Huang R, et al. Dynamic neuroimaging biomarkers of smoking in young smokers. *Front Psychiatry.* 2020;11:663.
12. Meng X, Zheng J, Liu Y, et al. Increased dynamic amplitude of low frequency fluctuation in primary insomnia. *Front Neurol.* 2020;11:609.
13. Zhang C, Dou B, Wang J, et al. Dynamic alterations of spontaneous neural activity in Parkinson's disease: a resting-state fMRI study. *Front Neurol.* 2019;10:1052.
14. Yan CG, Wang XD, Zuo XN, et al. DPABI: data processing & analysis for (Resting-State) brain imaging. *Neuroinformatics.* 2016;14:339–351.
15. Yin S, Liu L, Tan J, et al. Attentional control underlies the perceptual load effect: evidence from voxel-wise degree centrality and resting-state functional connectivity. *Neuroscience.* 2017;362:257–264.
16. Goto M, Abe O, Aoki S, et al. Diffeomorphic anatomical registration through exponentiated Lie Algebra provides reduced effect of scanner for cortex volumetry with atlas-based method in healthy subjects. *Neuroradiology.* 2013;55:869–875.
17. Yan CG, Cheung B, Kelly C, et al. A comprehensive assessment of regional variation in the impact of head micromovements on functional connectomics. *Neuroimage.* 2013;76:183–201.
18. Liao W, Wu GR, Xu Q, et al. DynamicBC: a MATLAB toolbox for dynamic brain connectome analysis. *Brain Connect.* 2014;4:780–790.
19. Liao W, Li J, Duan X, et al. Static and dynamic connectomics differentiate between depressed patients with and without suicidal ideation. *Hum Brain Mapp.* 2018;39:4105–4118.
20. Schrouff J, Rosa MJ, Rondina JM, et al. PRoNT: pattern recognition for neuroimaging toolbox. *Neuroinformatics.* 2013;11:319–337.
21. Liu F, Guo W, Yu D, et al. Classification of different therapeutic responses of major depressive disorder with multivariate pattern analysis method based on structural MR scans. *PLoS One.* 2012;7:e40968.
22. Baliki MN, Mansour AR, Baria AT, et al. Functional reorganization of the default mode network across chronic pain conditions. *PLoS One.* 2014;9:e106133.
23. Jones SA, Morales AM, Holley AL, et al. Default mode network connectivity is related to pain frequency and intensity in adolescents. *Neuroimage Clin.* 2020;27:102326.
24. Alshelh Z, Marciszewski KK, Akhter R, et al. Disruption of default mode network dynamics in acute and chronic pain states. *Neuroimage Clin.* 2018;17:222–231.
25. Liu P, Liu Y, Wang G, et al. Aberrant default mode network in patients with primary dysmenorrhea: a fMRI study. *Brain Imaging Behav.* 2017;11:1479–1485.
26. Zunhammer M, Busch V, Griesbach F, et al. rTMS over the cerebellum modulates temperature detection and pain thresholds through peripheral mechanisms. *Brain Stimul.* 2011;4:210–217 e211.
27. Claassen J, Labrenz F, Ernst TM, et al. Altered cerebellar activity in visceral pain-related fear conditioning in irritable Bowel syndrome. *Cerebellum.* 2017;16:508–517.
28. Jones AK, Brown WD, Friston KJ, et al. Cortical and subcortical localization of response to pain in man using positron emission tomography. *Proc Biol Sci.* 1991;244:39–44.
29. Xiao X, Ding M, Zhang YQ. Role of the anterior cingulate cortex in translational pain research. *Neurosci Bull.* 2021;37:405–422.
30. Orenius TI, Raji TT, Nuortimo A, et al. The interaction of emotion and pain in the insula and secondary somatosensory cortex. *Neuroscience.* 2017;349:185–194.
31. Apkarian AV, Sosa Y, Sonty S, et al. Chronic back pain is associated with decreased prefrontal and thalamic gray matter density. *J Neurosci.* 2004;24:10410–10415.
32. Dun WH, Yang J, Yang L, et al. Abnormal structure and functional connectivity of the anterior insula at pain-free periovulation is associated with perceived pain during menstruation. *Brain Imaging Behav.* 2017;11:1787–1795.
33. He J, Dun W, Han F, et al. Abnormal white matter microstructure along the thalamus fiber pathways in women with primary dysmenorrhea. *Brain Imaging Behav.* 2021;15(4):2061–2068.
34. Yang SQJ, Dun W, Wang K, Liu H, Liu J. Prediction of pain intensity with uterine morphological features and brain microstructural and functional properties in women with primary dysmenorrhea. *Brain Imaging Behav.* 2021;15(3):1580–1588.
35. Zhang J, Su J, Wang M, et al. The sensorimotor network dysfunction in migraineurs without aura: a resting-state fMRI study. *J Neurol.* 2017;264:654–663.
36. Niddam DM, Wang SJ, Tsai SY. Pain sensitivity and the primary sensorimotor cortices: a multimodal neuroimaging study. *Pain.* 2021;162:846–855.
37. Wei SY, Chao HT, Tu CH, et al. Changes in functional connectivity of pain modulatory systems in women with primary dysmenorrhea. *Pain.* 2016;157:92–102.

Journal of Pain Research

Dovepress

## Publish your work in this journal

The Journal of Pain Research is an international, peer reviewed, open access, online journal that welcomes laboratory and clinical findings in the fields of pain research and the prevention and management of pain. Original research, reviews, symposium reports, hypothesis formation and commentaries are all considered for publication. The manuscript

management system is completely online and includes a very quick and fair peer-review system, which is all easy to use. Visit <http://www.dovepress.com/testimonials.php> to read real quotes from published authors.

Submit your manuscript here: <https://www.dovepress.com/journal-of-pain-research-journal>